Armenian Journal of Physics, 2010, vol. 3, issue 4, pp. 312-341

LOW-FREQUENCY NOISES IN NANOTUBES AND NANOWIRES

Ferdinand Gasparyan

Department of Physics of Semiconductors & Microelectronics, Yerevan State University,
1 Alex Manoogian St., 0025 Yerevan, Armenia, Phone: (37410) 39 03 33, E-mail: fgaspar@ysu.am

Received 15 October, 2010

CONTENTS

VOCABULARY

1D – one-dimensional; 2D – two-dimensional; 3D – three-dimensional;

NT – nanotube; NW – nanowire;

CNT – carbon nanotube; s-CNT – semiconducting CNT;

SWNT – single-walled nanotube;

SWCNT – single-walled carbon nanotube;

MWNT – multiwalled carbon nanotube;

FET – field-effect transistor;

CNTFET – carbon nanotube field-effect transistor;

CVD – chemical vapor deposition;

MISFET – metal-insulator-semiconductor field-effect transistor;

NSD – noise spectral density;

SNR – signal-to-noise ratio;

RTS – random telegraph signal; RTN – random telegraph noise;

SB – Schottky barrier;

LED – light emitting diode;

SET – stepped electrode transistor

UV – ultraviolet;

MOS – metal – oxide – semiconductor;

d.c. – direct current;

g-r – generation-recombination;

hcp – hexagonal closely packed; fcc – face-centered cubic.

1. Introduction

While the noise is usually regarded as an undesirable property for applications, the fluctuation phenomenon in itself contains important information about the material and may be utilized as a valuable probe to characterize nanostructures. In NT devices, the 1/f-noise is found to be much more pronounced than in conventional bulk devices, and this may seriously limit the potential of NTs for applications in electronics. Excess noise, by which is meant noise above the unavoidable thermal Nyquist level, is a recognized barrier to practical, nanometer-scale devices since it usually increases dramatically as dimensions shrink [1]. Knowledge of the noise characteristics is important to characterize performance of NT and NW based devices.

It is now widely accepted that low-frequency (LF) noise is produced by fluctuations in sample conductance. In general, if diffusive transport is assumed, the conductance σ is proportional to both carrier mobility μ and carrier concentration n:

$$\sigma = e\mu n.$$

In principle, both n and μ can contribute to the 1/f-noise. Numerous LF noise models have been proposed for different types of materials [1-3] and they usually divide into two general categories, namely, number (Δn) and mobility ($\Delta\mu$) fluctuations models. Also, a combination and modification of both models applicable for many types of conventional FET and other semiconductor devices was proposed (see, e.g., [4-7]. Resistance measurements do not enable the identification of the source of the 1/f-noise. In contrast, by studying the gate voltage dependence of the noise associated with source-drain current in FETs, the contributions coming from fluctuations of n and fluctuations of μ can be separated [8]. NT and NW based devices have been shown to exhibit very significant current fluctuations in the LF regime [9], which may present serious limitations for device performance and applicability, e.g., the threshold voltage of a transistor and the detection sensitivity of a several type sensors. The ratio of electronic noise to device signal is expected to increase in devices of decreasing size [1] and is thus of concern in nanoscale devices. In addition, surface adsorbents [10] and atomic scale structural fluctuations [11] are expected to have increased influence on electronic noise as the surface to volume ratio increases.

There are reports on electronic LF noise in a metallic CNT [12], CNT ropes [9,13], and networks [9,14,15], individual s-CNTs [16], Si NWs [6,17,18], GaN NWs [1,19,20-22], ZnO and CdS NWs and nanobolts [23,24].

2. Carbon based NTs and NWs

Carbon NTs and NWs are promising candidates for advanced nanoelectronic devices, and they have demonstrated great potential in a wide range of applications, such as FETs [25-27], elementary logic circuits [28-31], and chemical sensors [9,32-34].

Both equilibrium and nonequilibrium fluctuations of a particular atom's location, for example, gain importance as conduction paths are reduced to atomic dimensions. CNTs, being covalently bonded metallic wires, might be less susceptible to such fluctuations. Furthermore, the strong carbon–carbon bonds which form the nanotube should not be subject to electromigration or defect propagation, two of the most important noise mechanisms in standard metal films and wires [19]. Since nanomaterials have been used for transport studies it has been frequently observed that their electrical characteristics showed substantial LF current fluctuations. Already in 2000 Collins et al. [9] classified those fluctuations in the case of CNTs as 1/f-type. Later works confirmed this finding [14-16,35,36]. For the back-gated CNT FET, it is known that source-drain current at fixed gate potential can drift in time due to significant NT-substrate interactions [37-39]. Such drift can introduce LF noise components greater than those from the NTs themselves.

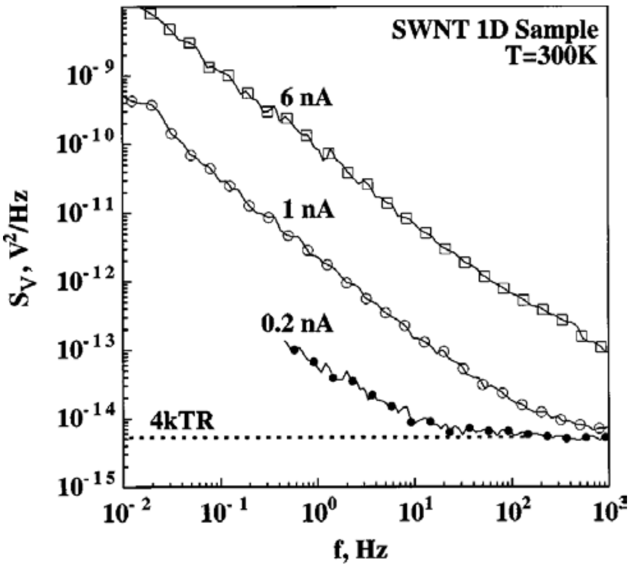

Fig. 1. Voltage noise power S_V vs frequency for a single SWNT, for three values of applied bias current. At low frequency, the noise greatly exceeds the thermal noise limit $S_V = 4kTR$. The SWNT has a two-probe resistance of 335 kΩ [9].

Various researchers have predicted both large and small amounts of 1/f-noise in CNT transistors. From one point of view, the strong carbon–carbon bonds in a CNT should reduce the amount of ion motion, which is a suspected source of 1/f-noise in other systems [19]. However, CNTs have the disadvantage of every atom being a surface atom, and are thus susceptible to the influence of adsorbents [40]. Additionally, due to the 1D electronic structure of the CNT, a local defect must globally affect the current. Roschier et al. [35] measured the charge sensitivity for a free-standing MWNT SET at sub-Kelvin temperatures and found noise properties equaling conventional metallic SET devices. Hence 1/f-noise does not present any problems when operating NT SETs at small currents were the squared current dependence of the noise power is still irrelevant.

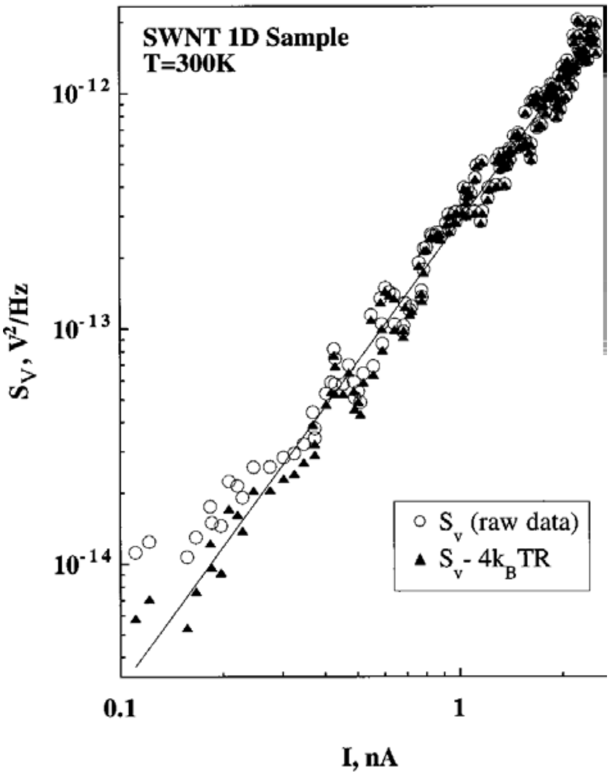

Fig. 2. Noise power S_V as a function of d.c. bias current for a SWNT. The closed circles represent the raw data, while for the open circles the bias-independent thermal noise has been subtracted. The excess noise fits an I^2 behavior. The measurement is performed at 0.3-10 Hz [9].

The room temperature noise characteristics of SWNTs in different configurations, ranging from isolated individual tubes to 2D ‘‘films’’ and 3D ‘‘mats’’ of randomly interconnected nanotube assemblies were studied in [9]. It find that all SWNT samples, irrespective of the contact electrode or tube connectivity configuration, display similar excessive 1/f-noise which cannot be explained within the idealized context of covalently bonded metallic wires. Figure 1 depicts the noise power at different bias currents measured across an isolated, single SWNT. At zero bias current, the noise was “flat” and agreed with the thermal Nyquist level $S_V = 4kTR$ (dashed line). At finite bias currents excess noise is observed. After subtracting the thermal baseline, the excess noise varies as $1/f^{\gamma}$, with $\gamma = 1.06 \pm 0.02$ for all bias currents within the linear-response regime. Excess SWNT noise is 1/f. A bias current dependence of the form I^{β} is found, with $\beta = 1.99 \pm 0.4$. To characterize the absolute amplitude of the excess noise the voltage noise power S_V is expressed as

$$S_V = A\frac{V^2}{f^{\gamma}}, \tag{1}$$

where $A = 1.0 \times 10^{-11} R$ at $\gamma = 1.06$. Voltage noise power as a function of d.c. bias current for a single SWNT is presented in Fig. 2. For an individual MWNT $S_V \propto V^{1.02}$. For low-crossing MWNT $S_V \propto V^{1.56}$ [20].

Unlike other types of noise, such as thermal noise or shot noise, which are not material-specific properties, parameter A generally reflects the sample quality and, most importantly, increases with decreasing device size [1]. For metallic NTs, Collins et al. have shown that the noise amplitude A is roughly proportional to the device resistance R [9]. In semiconducting NTs, A is further modulated by the gate voltage that varies the device resistance, showing an experimental dependence $A \propto 1/N$, where N is the number of atoms or carriers in the system and find that Hooge's empirical rule adequately describes the LF noise in s-CNT FETs with $\alpha_H = (9.3 \pm 0.4) \times 10^{-3}$ [16]. A linear increase of noise level with resistance can be understood if the samples consist of several parallel conduction channels. In this case the resistance is inversely proportional to the number of channels M, while 1/f-noise spectral density, according to Hooge's empirical formula [1-3]

$$S_I = \alpha_H I^2 / N f^{\gamma} \text{ or } S_V = \alpha_H V^2 / N f^{\gamma} \quad (2)$$

scales as $\propto 1/N$, where N is the number of free charge carriers proportional to system size. As $N \propto M$, it follows that $S_I \propto R$. This reasoning applies to a selection of samples, in which the conductivity is determined by the number of parallel conduction paths. On the contrary, one would expect the resistance to be directly proportional to sample length L, as well as $N \propto L$, which would give $S_I \propto 1/R$. Such dependence is not observed.

High-quality metal films tend to have values of A as small as 10^{-19}, with values increasing to 10^{-17} for thin films with strong grain boundary effects. Carbon composite resistors considered unsuitable for most low-noise circuitry, have excess noise amplitudes between 10^{-15} and 10^{-13} (for $R \leq 1\text{k}\Omega$). Carbon fibers with resistances $\leq 1\text{k}\Omega$ show similar noise magnitudes. Hence, 1/f-noise in SWNT conductors is four to ten orders of magnitude larger than that observed in more conventional conductors. Low 1/f-noise, $A \approx 10^{-13}$, was recorded for a thick rope of SWNTs [13]. At a very large current, $I = 0.1\text{mA}$, $A \approx 10^{-10}$ has been observed for a MWNT, but that value is not likely to extrapolate well down to low currents [41].

What is the origin of the excess noise in SWNTs?

The expected noise immunity of a covalently bonded system is in competition with the increased relative importance of individual atomic fluctuations in nanometer-sized junctions. This size scaling is incorporated in Hooge's empirical law, which expresses the excess noise magnitude as

$$A = \alpha_H / N, \quad (3)$$

$\alpha_H = 0.002$ is a constant. Hooge's law holds true for most bulk metallic systems, and even extends to the $N = 1$ case at the tip of a scanning tunneling microscope. Estimating for the SWNT of Fig. 1

$N \sim 10^4$ atoms gives an estimate $\alpha_H = 0.2$ for SWNTs, in sharp disagreement with Hooge's law. In semiconductors and very small metal whiskers, where surface and impurity fluctuations can dominate typical bulk effects, α_H may be substantially larger than 0.002. The large value of α_H observed for SWNT similarly suggests an important role played by surface fluctuations, a result not totally unexpected if one considers that every atom that constitutes a SWNT is a surface atom. As is shown in [9], A scales with R can also be illuminated by Hooge's law. Combining $A = 10^{-11} R$ with Hooge's law gives $A = \alpha_H / N = 10^{-11} R$, whereby the number of carriers N is simply proportional to the sample conductance $G = R^{-1}$. From a qualitative point of view, this relationship merely reflects that both N and G depend on the number of parallel, conducting SWNTs in the sample.

A less desirable property of CNT-based electronic devices is that they exhibit a large component of 1/f-noise. Collins et al. [9] have shown that a wide variety of single- and MWCNT devices, including individual SWNTs, 2D-networks, and 3D-mats of NTs, all exhibit a large value of 1/f-noise that is proportional to the device resistance. This large value of 1/f-noise is not surprising given that the electrical current in NTs is transmitted through surface atoms and is easily perturbed by local charge fluctuations. Because the magnitude of this noise is orders of magnitude larger than the noise observed in more conventional electronic materials 1/f-noise is an important consideration in assessing the potential of CNTs for electronic and sensor applications. Based on their measurements on SWNTs, Collins et al. [9] present an empirical model according to which the noise level is directly proportional to the sample resistance. The model was confirmed by Snow et al. [14] for 2D SWNT mats and in addition a direct dependence on size was found. Investigations of SWNT devices in [14] show that devices with similar resistances but with different sizes exhibit a systematic variation in the magnitude of 1/f-noise. In particular, in [14] observe that the level of 1/f-noise in large-area devices is significantly less than the level of noise in small-area devices of comparable resistance. The investigated devices in [14] consist of electrically continuous 2D-networks of SWNTs. The SWNTs were either grown directly on the thermal oxide (200 nm thick) of a Si-substrate using CVD or deposited onto the substrate from an aqueous 1% sodium dodecyl sulfate solution of suspended SWNTs. The conducting Si substrate was used as common back gate. The width of the electrodes (W) and their spacing (L) was varied from 3 mm to 1 cm with aspect ratios (L/W) ranging from 1 to 0.02. The resistance of low-resistivity networks scales as L/W; however, the higher resistivity films display nonlinear scaling. According to Hooge, A depends on the number of charge carriers in the conductor N through Eq. (3) where $\alpha_H = 2 \times 10^{-3}$ [1]. Although it is now understood that the γ value is not universal, it is a good starting point to compare the magnitude of noise in NTs to that in bulk conductors described by Hooge's law. The NTs described in [14] contain about 2000 conduction electrons (this estimate is for the NT with a length of 500 nm). Using the magnitude of A found above, in [14] the authors found $\alpha_{H,NT} \approx 4\times10^{-3}$.

In [42] discussed the dependence of the SNR on gate potential and device architecture, and show that it can be related to fluctuations in the gate-independent device resistance.

Results of measurements of LF current noise in five arc-discharge-grown MWNTs were reported in [43]. The NSD have been recorded at temperatures of 295K, 77K, and 4.2K, and find that the noise level decreases moderately with temperature. At liquid helium temperatures, instead of the usual 1/f-type of spectra, authors observed Lorentzian line shapes resulting from one or a few systems of two-level fluctuations, analyzed these spectra in terms of resistance fluctuations ΔR and obtained $\Delta R = 1$ kΩ, most likely caused by changes in the contact resistance. Single NTs approximately 20 nm in diameter and 1 μm in length, were positioned across a gap between two wide and pre-patterned gold electrodes. At 295 and 77 K the NSD can be accounted for by the formula

$$S_I = A\frac{I^\beta}{f^\gamma}. \tag{4}$$

The values of exponents β and γ are given in Table for the 5 samples.

Table: Exponents β and γ, and inter-extrapolated NSD at $f_0 = 100$ Hz and $I = 100$ nA [43]

Sample	$R_{295\text{K}}$ (kΩ)	S_I(295K) (pA^2)/Hz	$\gamma_{295\text{K}}$	$\beta_{295\text{K}}$	$R_{77\text{K}}$ (kΩ)	S_I(77K) (pA^2)/Hz	$\gamma_{77\text{K}}$	$\beta_{77\text{K}}$	$R_{4\text{K}}$ (kΩ)	S_I(4K) (pA^2)/Hz
1	33	8	1.07	2.28	53	6	1.03	2.00	55	1
2	390	40×10^3	1.09	1.76	2450	2×10^3	1.09	1.54	620/910a	300
3	133	200	1.15	2.04	801	8	1.16	2.12	275	1
4	-	-	-	-	70	20	0.94	1.87	106	1
5	13	90	1.07	1.93	26	20	b	1.79	49	4

[a]The differential resistance is asymmetric with respect to the current direction.
[b]The experimental value was not determined. $\gamma = 1$ was assumed for extrapolation.

The linear resistance is given for 295K and 77 K, while the 4K value is the differential resistance at 100 nA. It is clear that $\beta = 2$ is expected for pure resistance fluctuation in ohmic conductors. The $\beta \neq 2$ behavior is associated with nonlinear characteristics, and the fact that $\beta < 2$ suggests S_I/I^2 scales proportionally to the resistance. It is find that at 4.2 K the 1/f-structure of Eq.(1) cannot account for the data anymore. Instead, the measured noise spectra are composed of a sum of a few Lorentzian line shapes:

$$S_I = I^2 \sum \frac{S_L^{(i)}\tau_i}{1+(2\pi\tau_i f)^2},$$

where each Lorentzian is characterized by a lifetime τ_i and an amplitude $S_L^{(i)}$. Those Lorentzians are found to depend on the bias voltage, which leads to irregular and nonmonotonic current dependence of the noise. According to the generic 1/f-model, the individual fluctuations are thermally activated, and freeze out, as the temperature is lowered. The two parameters characterizing an individual fluctuator, the magnitude S_L and the life time τ, were both found to depend on the bias current. Eventually, so few sources are left that they show up as individual Lorentzians. The noise scales as

$$S_I \propto kD(E), \tag{5}$$

where $D(E)$ is the distribution of the activation energies and

$$E = -kT\ln(2\pi f \tau_0), \tag{6}$$

where τ_0^{-1} is the attempt frequency [44]. Assuming weakly energy-dependent $D(E)$, the examined samples in [43] full quite close to this model. Using the value $A = S_I f / I^2$ (which a weak function of I and f) in [43] at 295 K $A = 8\times10^{-8} \div 4\times10^{-4}$. This is comparable to $A = 3\times10^{-7}$ reported for a MWNT [20]. Note that for individual SWNTs $A \approx 10^{-5}$ [9] and $A = 3\times10^{-5}$ [12].

The dependence of S_I (or A) on the gate voltage [15,16,45], NT length [16,56], the substrate on which the SWNT rests [47] and the contact metal has been discussed. The majority of these studies compare experimentally measured noise magnitudes in SWNT-FETs [9,16,45,47-49] to the empirical Hooge model [1,3]. Hooge model suggests that noise is caused by independent scattering events of charge carriers, which lead to $1/N$ dependence. Tersoff [50] has proposed an alternative model that assumes that the SWNT-FET is affected by random fluctuation of charge in its environment. In this "charge-noise model"

$$S_I \propto \left(dI/dV_g\right)^2, \tag{7}$$

$$A \propto \left(d\ln I/dV_g\right)^2. \tag{8}$$

In [5] a reliable set of experimental data was collected to compare to these two models. SWNTs were grown by CVD onto Si wafers with a 500 nm thick SiO_2 layer. SWNT diameters were 2.0 nm and contacted with Au top electrodes with a 2.0 nm underlayer of Cr. Channel length was below 100 nm. In [5] note two properties of N that hold irrespective of the ballistic or diffusive nature of electronic transport in SWNTs: (i) N, and thus $S_I(1\text{Hz})/I^2$, as a function of liquid-gate voltage follows an exponential law in the subthreshold region with the same exponential slope as the source-drain current [50], and (ii) N scales with the channel length as $N \propto L$ at fixed gate voltage. Comparison shows that the Hooge model fails to describe the experimental data. In [5] note that all devices yield remarkably comparable A values that are quite independent of the channel length, except for the shortest device in the subthreshold region. Authors conclude also that the charge-noise model presents an accurate description of experimental data in the threshold regime of SWNT-FETs. The level of charge-noise is higher for SWNT-FETs with short NT lengths. It appears that

$$S_I(1\text{Hz}) \propto S_{input}\left(dI_{sd}/dV_{\text{lg}}\right)^2, \tag{9}$$

and $S_{input} \propto 1/L$. Here V_{lg} is the electrolyte potential. This dependence explained as follows. In the charge-noise model the voltage fluctuations of the gate, described by the proportionality constant S_{input}, are the result of charge fluctuations. These fluctuations couple to the SWNT-FET through some effective gate capacitance, C_{gate} so that

$$S_{input} = \left(dV_{\text{lg}}/dq\right)^2 S_q = \left(1/C_{gate}\right)^2 S_q\,. \tag{10}$$

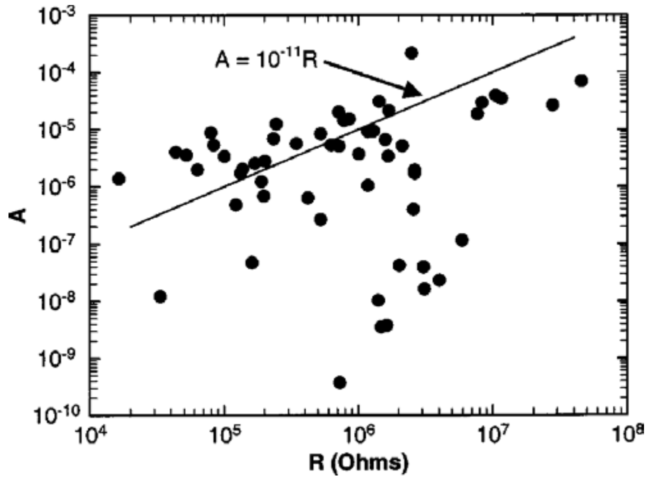

Fig. 3. Plot of the scaled noise $A = fS_V/V^2$, measured in 2D networks versus the device resistance [14]. The solid line corresponds to the empirical relationship established in [9].

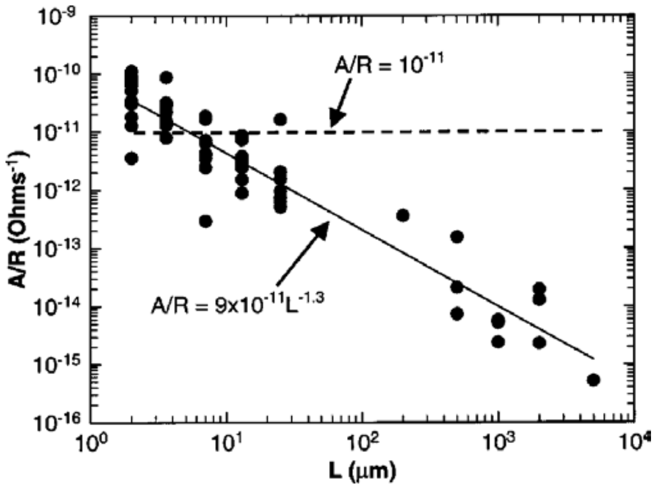

Fig. 4. The same data as in Fig. 3 plotted as A/R versus the electrode spacing L [14]. The dashed line represents $A/R = 10^{-11}$ [9] and the solid line is a least-squares power-law fit to the data. A clear relationship between the level of 1/f-noise and the device size is established.

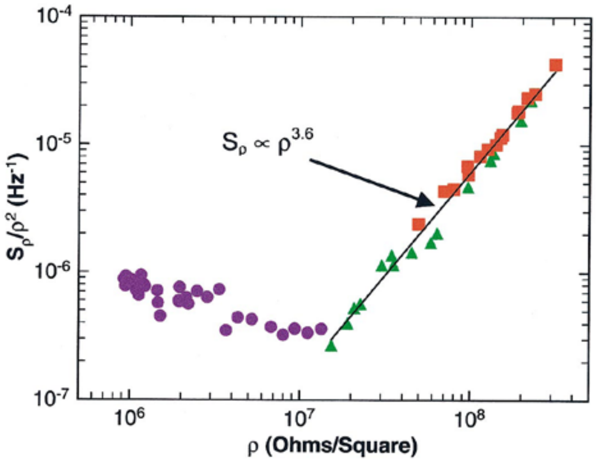

Fig. 5. The circles correspond to $V_g < 0$, the triangles to $0 < V_g < 1.6$ V, and the squares to $V_g > 1.6$ V. As the gate bias shuts off the current in the network, the noise increases as a power law of the resistance. This behavior is similar to the 1/*f*-noise scaling observed in percolating systems [14].

The effective gate capacitance scales as $C_{gate} \propto L$ and is presumably dominated by the quantum capacitance [51]. On the other hand, a homogeneous distribution of independent charge fluctuations along the length of the SWNT leads to $S_q \propto L$. Combining these dependences for C_{gate} and S_q gives $S_{input} \propto 1/L$. This dependence also excludes that charge fluctuations in the SWNT-metal contacts are the dominating source of noise. Tersoff has proposed to include an extra term in the noise expression similar to the Hooge model

$$S_I = S_{input}\left(\frac{dI}{dV_{\lg}}\right)^2 + AI^2 . \tag{11}$$

In [14] authors confirmed the V^2/f scaling of the LF noise for the 2D-network devices, which consist of a large number of intersecting SWNTs. This behavior contrasts the scaling observed between two crossed MWCNTs that deviate significantly from the V^2/f behavior [20]. Using the $f = 10$ Hz noise in [14] take the approach of Collins et al. and plot the scaled noise, $A = fS_V/V^2$, versus device resistance (see Fig. 3). The solid line in Fig.3 is a plot of $A = 10^{-11}R$. While there is a general agreement between the level of noise for those devices and the noise levels observed by Collins et al., the data indicate that the resistance value alone is insufficient to predict the level of 1/f-noise. The reason that the 1/f-noise magnitude in devices discussed in [14] does not correlate well with the resistance is that the devices were constructed using a wide range of sizes. So, the device size is an important additional component in predicting the magnitude of 1/f-noise. In order to observe this size dependence in [14] plot the same data set as A/R versus the electrode spacing L (Fig. 4). A least-squares power-law fit of the data (solid line) yields $A/R = 9\times10^{-11}/L^{1.3}$, where L is in units of mm. The resulting empirical formula

$$S_V = 9\times10^{-11}\frac{R}{L^{1.3}}\frac{V^2}{f} \qquad (12)$$

is a good predictor of the LF noise in SWNT networks ranging in resistance from $10^4 \div 10^7\,\Omega$ and spanning device areas from 10 to 108 μm^2. From this formula it is clear that for low-noise applications such as sensing that large-area SWNT devices will produce superior noise performance to nanometer-scale sensors. For comparison, this expression predicts that a 1mm-sized, 1 MΩ SWNT sensor biased at 10 nA will exhibit 1/f-noise in excess of the background thermal noise $(S_V = 4kTR)$ for $f < 70\,$Hz. The reduction of the 1/f-noise with device size is consistent with other electronic systems in which the magnitude of the 1/f-noise varies inversely with the number of charge carriers N in the device. According to this behavior, the 1/f-noise should scale as R/L^2, i.e.

$$\frac{R}{L^2} = \frac{1}{e\mu N}.$$

The R/L^2 behavior assumes a uniform system of uncorrelated noise sources that number in proportion to N. In contrast, the SWNT network consists of many parallel one-dimensional paths formed by intersecting SWNTs. The SWNTs consist of a mixture of both metallic and semiconducting NTs that have large variations in resistance, which results in nonuniform voltage drops along the conduction paths. Thus, the dominant noise sources will occur at the high-resistance segments of the current paths. The source of gate-induced noise is not understood, but authors note that field-induced charge fluctuations in the gate oxide are one possible cause. As note in [14] the gate field might also produce charge fluctuations in the SiO_2 gate dielectric that increases the level of 1/f-noise. In Fig. 5 the normalized resistivity fluctuations $S_\rho/\rho^2\ (\equiv S_V/V^2)$ versus resistivity ρ is presented.

In [52] LF noise measurements have been performed on a SWCNT connected by Ti/Au electrodes. It has been found that the 1/f-noise decreases when the measurements are undertaken under vacuum and when the NT is partially degassed, showing a correlation between the fluctuation inducing the 1/f-noise and the presence of gases. It is shown that the 1/f-noise sources are located at the metal/NT contacts. It was shown that parameter A appears to be proportional to the sample resistance by a proportionality factor close to $10^{-11}\,\Omega^{-1}$. As noted in [52], result $A = 1.0\times10^{-11}R$ may seem surprising as the transport is ballistic in individual NTs and diffusive in films or mats. Snow et al. [14] have shown that for films A is inversely proportional to the dimensions of the bulk but remains proportional to $10^{-11}\,\Omega^{-1}$. Nevertheless other results [12,43] have shown A to be dependent with resistance for individual NTs. In [52] it was also shown that when the device is under vacuum, the effects of gases are reduced and A decreases. Ambient gases can be considered to be at the origin of the fluctuations leading to the 1/f-noise. Excess noise with a slope different from unity can be explained by a superposition of a few Lorentzians and of the 1/f-noise. The change in slope with respect to temperature is thus explained by the variation of trap activities. Lorentzians are associated to defects or strongly bounded molecules remaining on the NT surface.

Investigations of LF current fluctuations of nanodevices consisting of one single semiconducting NT were shown that the device current diminishes with increasing V_g, and the noise amplitude A increases monotonically with the device resistance R, with an A/R ratio that lies between 2×10^{-10} and $2\times10^{-9}\,\Omega^{-1}$ [15]. On the basis of the statistics of a large number of devices consisting of mixtures of different types of CNTs (i.e., 2D mats and 3D networks), it has been concluded that the 1/f-noise amplitude in these CNT-based devices increases with the sample resistance R with the A/R ratio depending on device dimensions [14]. In [15] find also that while Eq. (3) holds true for most bulk and thin film specimens with diffusive transport behaviors, there has been no experimental verification of the relation and/or information about α_H for 1D systems exhibiting quasi-ballistic transport behavior. Results of [15] present strong evidence that the gate-dependent 1/f-noise observed in CNs is modulated by the total number of transport carriers in the channel according to Eq. (3), and the fluctuation mechanism is independent of the carrier type, i.e., electrons or holes. Furthermore, the 1/f-noise parameter determined for the CNFETs that consist of unpurified CNTs is quite comparable to the value observed in most bulk systems. The much larger $\alpha_H = 0.2$ deduced in [9] is due to an overestimation of N by adopting the number of atoms instead of the number of transport carriers, as well as the lack of a quantitative model to accurately extract N. To further demonstrate the N dependence and to evaluate the significance of scattering on the 1/f-noise of NTs, in [9] fabricated two SB-CNFETs with very different channel lengths: $L \approx 500$ nm and 7 μm, which are denoted as short (S) and long (L) devices, respectively. To eliminate device-to-device variations, the two CNFETs are fabricated using one, single, long semiconducting NT and share a common electrode as the source. The ratio of the noise amplitude $A_S/A_L \approx 10$ of the two devices is comparable to the inverse of the corresponding length ratio $L_S/L_L = 14$, consistent with $A \propto 1/N \left(\propto 1/L\right)$ behavior. Taking into account this length dependence, the CNFET resistance can be expressed as [9]

$$R = R_{SB} + R_{diff} = R_{SB} + R_0 \frac{L}{\lambda}, R_0 \equiv \frac{h}{4e^2}, \tag{13}$$

where λ is the electron mean-free-path in the CNT and R_{SB} and R_{diff} are the resistance contributions due to the contact Schottky barriers and the scattering within the NT channel, respectively, R_0 is the theoretical tube resistance at the ballistic limit $\left(\sim 6.5\,\mathrm{k\Omega}\right)$. Although it has been suggested that the 1/f-noise in bulk materials is induced by scattering with surface or/and bulk phonons [6,7,53-62] and the same may be true for NTs [18,63]. The agreement between A_S/A_L and L_S/L_L is striking and suggests that α_H in CNFETs is not substantially influenced by the presence of acoustic phonon scattering in the long channel device.

In [64] the results of Monte-Carlo LF noise simulations as a function of film thickness, width and length were presented and compared with experimental data. To model to physical properties of the film, the resistance of an individual NT is calculated by

$$R_{CNT} = R_0 \frac{L}{\lambda}.$$

For computing the 1/f-noise in the CNT film in [64] used a model which takes into account the noise contributions from both the NTs themselves and the tube-tube junctions in the film and assumed $\lambda \approx 1\,\mu\text{m}$. Assuming independent noise sources the relative 1/f-noise magnitude of the film, A_{eq}, can be written as

$$A_{eq} = \frac{S_I f}{I^2} = \frac{1}{V^2 I^2} \sum_n i_n^4 r_n^2 A_n \,, \tag{14}$$

where i_n is the current, A_n is the relative 1/f-current noise amplitude, and r_n is the resistance of the tube or junction associated with the *n*-th individual noise source. Based on experimental results in [96] were used $A_n = 10^{-10} R_0/L$ for the 1/f-noise amplitude of individual NTs, where L is expressed in microns and $R_0 = 6.5\,\text{k}\Omega$ [15]. Based on experimental data a relationship $A_n = a r_n$ was assumed with $a = 10^{-10}\,\Omega^{-1}$. The simulation results are in excellent agreement with the experimental data of [14], clearly indicating that

$$\frac{A}{R} \propto L^{\alpha}$$

is a strong function of device length with a critical exponent $\alpha = -1.3$ (for $8 < L < 20$ μm). The decrease in the noise amplitude with device length is consistent with Hooge's law, where $A \sim 1/N$. However, since the resistance of the CNT film device is given by $R = \rho L/Wt$, where N scales with the device volume, i.e. $N \sim LWt$, A/R is expected to scale as $A/R \sim L^{-2}$. For $W > 2$ μm A is inversely proportional to W ($\sim W^{-1.1}$). For $W < 1$ μm there is a strong power-law relationship between A and W ($\sim W^{-5.6}$). This shows that the variation of resistivity has a strong effect on the noise. In [96] the noise relative amplitude normalized by thickness, $A \times t$ were used (because A varies with thickness linearly in the regime when resistivity is constant). The simulation data can be fit by $A \times t \sim \rho^{\nu}$, where the extracted critical exponent is $\nu = 1.8$.

Two microscopic charge transport mechanisms occur in the films: the transport along NT themselves and the transport between crossed NTs. Considering the large mean free path in CNTs and the weak coupling between NTs, in [66] assume that the contacts between NTs dominate the transport through the film. From a macroscopic point of view, the NT film is modeled as a percolation network. Percolation networks have electrical properties that vary rapidly in the vicinity of the percolation threshold and follow power laws related to the density of NTs. The conductivity and noise coefficient A was measured for the different densities. These two quantities follow power laws with critical exponent t_c for the conductivity and k for the noise, as expected in percolation processes:

$$A \propto \left(\frac{RS}{L}\right)^{w}, \tag{15}$$

where $w = k/t_c$, R is the film resistance, S the section area. This expression explains the different empirical relations found in [14].

About the generating mechanism of 1/f-resistance fluctuation, there is an opinion that it is caused by the mobility fluctuation, and there is also an opinion that it is caused by the fluctuation of carrier density. In [67] the resistance fluctuation of CNTs in vacuum low temperature with laser irradiation was measured and the origin of mobility fluctuation was suggested. The resistance fluctuation remarkably increases and the fluctuation of the Schottky barrier was not the main origin of 1/f-resistance fluctuation. From the comparison of the experiments and the simulation it was thought that the main cause of 1/f-resistance fluctuation is the mobility fluctuation by lattice vibrations.

In [12] reported a characterization of the LF electronic noise properties of individual metallic SWCNT. The frequency dependence follows Hooge's law. Here study the charge sensitivity of an intramolecular CNT single-electron transistor. The NSD has been measured for individual NTs as a function of the d.c. current I_{DC} at room temperature. At $I_{DC} = 0$, the voltage noise is white and equals the expected value for thermal noise $4kRT = 2.1\times10^{-16}$ V^2/Hz of the nanotube, where $R = 12.6$ kΩ for this device. With increasing current, additional noise appears which exhibits 1/f-frequency dependence. These two noise powers appear to add incoherently, i.e.

$$S_V = 4kRT + \frac{B}{f}. \tag{16}$$

It is found that $B = AV_{DC}^2$. It is often convenient to assume that

$$S_{V,1/f} \propto \frac{V^2}{f} \text{ or } S_{I,1/f} \propto \frac{I^2}{f}.$$

In general, however, it is found that

$$S_{1/f} \propto \frac{V^{2+\delta}}{f^{1+\eta}},$$

where $|\delta| << 1$, and $|\eta| << 1$ are material dependent numbers.

In [16] the 1/f-noise in individual s-CNT in a FET configuration has been measured in ultrahigh vacuum and following exposure to air. The amplitude of the normalized current NSD is independent of source-drain current and inversely proportional to gate voltage, to channel length, and therefore to carrier number, indicating that the noise is due to mobility rather than number fluctuations. Hooge's constant for s-CNT is found to be $(9.3\pm0.4)\times10^{-3}$. The magnitude of the 1/f-noise is substantially decreased by exposing the devices to air. It was found that the 1/f-noise decreases when the same devices are subsequently measured in air. The s-CNTs used in this experiment were grown from iron-based catalysts by chemical vapor deposition on thermally grown SiO_2 on degenerately doped Si substrates. Electron beam lithography was used to define Cr/Au electrodes in a two-probe configuration with channel lengths of 1.6–28 µm. In the linear I-V regime, described in [16], 1/f-noise changed according (3), with $\beta = 2$ and $\gamma = 1$. In experiment in [16] typically find $S_I \propto I^{2\pm0.1}$. The frequency dependence of the noise reveals two types of LF noise spectra. For the first type the inverse of the normalized noise power is proportional to the frequency; i.e., electronic noise in the first type of spectrum is strictly 1/f. For the second type a minor deviation from 1/f dependence can be due to RTS often present in NT FETs [68] and submicron CMOS FETs. It is generated by the trapping-detrapping of carriers by tunneling into traps in SiO_2 [37, 68]. The deviation observed can be well explained by the addition of a g-r noise term [23] which adequately describes RTS,

$$S_I = \frac{AI^2}{f} + \frac{BI^2}{1+(f/f_0)^2}, \tag{17}$$

where f_0 is the characteristic frequency for the g-r noise. For the case of mobility fluctuations, Hooge's empirical rule states that the noise coefficient A is given by Eq. (3). Since the total number of carriers in the system $N = C_g L|V_g - V_{th}|/e$ in a one-dimensional FET in the on state, the above equation may be rewritten as

$$\frac{1}{A} = \frac{C_g L|V_g - V_{th}|}{e\alpha_H}, \tag{18}$$

where V_d, V_g and V_{th} are the drain voltage, gate voltage, and device threshold voltage, respectively. The gate capacitance per length C_g is given by [69]

$$C_g = \frac{2\pi\varepsilon_0\varepsilon_{av}}{\ln(2z/d)}, \tag{19}$$

where ε_{av} is the average dielectric constant of the gate dielectric and the medium above the CNT, z is the thickness of the gate dielectric, and d is the diameter of CNTs.

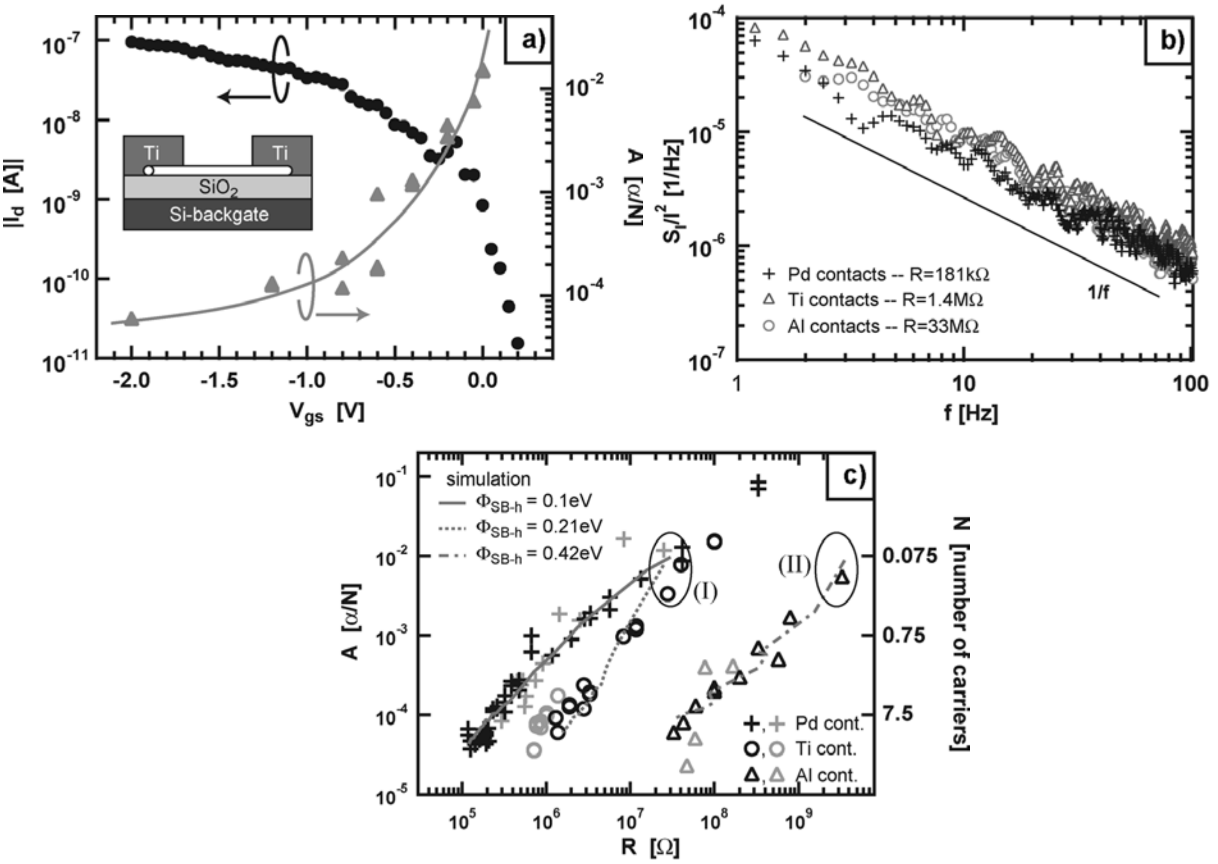

Fig. 6. (a) Device current I_d and noise amplitude A at $V_{ds} = -0.1$ V as a function of gate voltage for a Ti-contacted sample. The gray line is a guide to the eyes. (b) Normalized current NSD as a function of frequency in the devices on-state for the three different contact metals used. (c) Noise amplitude A as a function of sample resistance for CNFETs of type A with three different contact metals. Black and gray symbols refer to different transistors respectively. The lines show the results of simulations using the extended Schottky barrier model [49].

There are two classes of models for 1/f-noise in MOSFETs [70]. Models based on mobility fluctuations predict that α_H is independent of gate voltage, while

$$\alpha_H \propto 1/\left|V_g - V_{th}\right|$$

in models based on number fluctuations. As such, in the linear regime,

$$1/A \propto \left|V_g - V_{th}\right|$$

if noise is due to mobility fluctuations and

$$1/A \propto \left|V_g - V_{th}\right|^2$$

if noise is due to number fluctuations. The amplitude of 1/f-noise is inversely proportional to $\left|V_g - V_{th}\right|$ indicating mobility fluctuations and ruling out number fluctuations as the cause. The amplitude is also inversely proportional to the device length demonstrating that the noise is a property of the length-dependent resistance of the CNT and not the electronic contacts.

The 1/f-noise in various ballistic CNT devices reported in [49].

In [15] found that the excess noise in CNTs is not higher than in other materials, e.g., silicon, and is related to the small number of carriers inside the tube. In [71] presented a study that evaluates the 1/f-noise in a ballistic, 1D system, i.e., an s-CNT, as a function of metal contact material and sample geometry in a FET layout. The 1/f-noise amplitude is obtained using $A = S_I f / I^2$. The distance between the source and drain electrode is around $L = 600$ nm for transistors.

For CNFETs made from 10 to 30 μm long chemical vapor deposition NTs the contact separation is around $L = 200$ nm. A gate controls the electrostatics inside the NT channel in the case of the laser ablation and arc-discharge tubes through a backside $t_{ox} = 10$ nm SiO_2 layer [49] [see Fig. 6(a)]. For the CVD grown tubes a similar gate control is obtained through a $t_{ox} = 15$ nm thick alumina film.

Investigations in [47] show that the 1/f-noise amplitude is reduced by about one order of magnitude when the NT is suspended. This result unambiguously confirms the oxide substrate as the major source of 1/f-noise in SWNT devices and provides insight into schemes to reduce the 1/f-noise in CNT devices. Authors assume that the 1/f-noise is dominated by the trapped charges in the oxide. LF noise spectral density is expressed by $S_I = AI^2 / f$. The large 1/f-noise level in SWNT devices is associated with the small number of carriers in the system (see also [16,72]), and for s-CNTs the noise amplitude may also be influenced by the Schottky barrier at the contacts [50]. In either case, trapped charges in the oxide have been suggested as one possible source for the 1/f-noise, where the trapping–detrapping of carriers changes the number of carriers in the channel and also varies the surface potential along the NT.

LF noise in a capacitive field-effect Al-p-Si-SiO_2-Ta_2O_5 EIS (electrolyte-insulator-semiconductor) structure functionalized with a polyaminoamide (PAMAM)/CSWNT multilayer has been investigated and compared with the noise in a bare EIS device [18,109]. The noise spectral density exhibits $1/f^{\gamma}$ dependence with the power factor of $\gamma \approx 0.8$ and $\gamma = 0.8 \div 1.8$ for the bare and functionalized EIS sensor, respectively. The gate-voltage NSD was practically independent on pH value of the solution, and is increased with increasing the gate voltage or gate-leakage current. It has been observed that the existence of the PAMAM/SWNTs multilayer leads to an essential reduction of 1/f-noise. The gate-current noise behavior in bare and functionalized EIS devices has been modelled using the flat band-voltage fluctuations concept. The experimentally observed gate-voltage dependence of the noise in capacitive EIS structures can be explained by the gate-voltage-dependent changes in the occupancy of the oxide trap levels resulting in a modulation of the conductivity of current paths or charge carriers passing through the EIS structure. Generally noise determined by the modulation of semiconductor depletion region capacitance and surface potential due to charge fluctuation at the insulator/electrolyte interface. Modified charge fluctuation noise model also successfully used for explanation of noise peculiarities of p-Si/SiO_2/Ta_2O_5/electrolyte and p-Si/SiO_2/Ta_2O_5/dendrimer/CNT/electrolyte (bio-)chemical sensors [110]. For NSD the following expression is obtained

$$S_V = \left(e^2 N_{ot} / wlC_{eff}^2\right)(1/f).$$

Here w and l are the gate width and length, N_{ot} is the equivalent density of traps per unit area at the SiO_2/electrolyte interface, C_{eff} is the cumulative effective capacitance.

While the current fluctuation generated by each trapping–detrapping center takes the form of RTS [68], the superposition of such RTS noises with a wide distribution of switching time constants yields the 1/f-noise spectrum. Before the etching, the current power spectra of investigated devices all exhibit the f^{-1} dependence with similar A values of 6×10^{-5}, 6×10^{-5}, and 8×10^{-5}.

It is shown that the 1/f-noise in single CNT-FETs is strongly dependent on temperature between 1.2 and 300 K [73]. Authors used the model of Dutta et al. [44] to extract the distribution of activation energies of the fluctuators $D(E)$, which shows two features: a rise at low energy with no characteristic energy scale, and a peak at energy of order 0.4 eV. The magnitude of the peak energy rules out physisorbed gas molecules with low binding energy, and electronic excitations or structural fluctuations of the CNT itself, as sources of room temperature noise. The gate voltage dependence of the noise additionally rules out potential fluctuations resulting from charge trapping and detrapping in the gate dielectric. The likely sources of the noise are the motion of defects in the gate dielectric or at the CNT-dielectric interface, or possibly strongly physisorbed (binding energy ~0.4 eV) species on the CNT or dielectric surface. The dependence of the noise on the reciprocal of the number of carriers in the sample is taken as evidence that the 1/f-noise originates in the bulk rather than on the surface; since N scales with volume Ω, the noise power $S_I \propto 1/\Omega$. However, in a 1D system such as CNTs, N is proportional to the length of the system; no useful distinction can be made between the surface area and the volume, hence no distinction between surface and bulk origins of the noise can be made from the N dependence. Originally Hooge proposed the α parameter in his equations to be a universal constant for semiconducting systems with $\alpha(T = 300\text{K}) \approx 2\times10^{-3}$. $\alpha(T)$ can vary as a result of sample preparation, material, defect density, and other effects [3]. In [73] used Hooge's relation simply as an empirical rule for characterizing the magnitude of the noise by a single (temperature-dependent) parameter $\alpha(T)$. Experiments showed that $\alpha(T = 300\text{K})$ is the same for NTs from 1 to 30 μm long, and indicate that the fluctuating resistance responsible for the 1/f-noise is indeed from the length-dependent diffusive resistance of the NT channel, not the contact resistance. Samples investigated in [73] are made using CVD grown CNTs, and contain single NTs contacted by Pd/Nb leads. The devices were above a layer of 400 nm of thermally grown SiO_2 with a heavily doped Si substrate to allow for back gating of the devices down to cryogenic temperatures. Here present data from two devices taken in a gas flow helium cryostat, with temperatures ranging from 1.2 to 300 K. Device 1 has a diameter 1.4 nm, and device 2 has a diameter of 1.9 nm. The devices each have a length of 3 µm. The number of carriers is determined by assuming that the device is in the linear regime. This gives the number of carriers to be linearly proportional to the gate voltage:

$$N = \left|V_g - V_{th}\right|\left(C_g / e\right),$$

where C_g is the capacitance of the CNT to the gate electrode, V_g the gate voltage, V_{th} the threshold voltage. The gate capacitance is determined by modeling the CNT as a wire over a two dimensional plane: $C_g = 2\pi\varepsilon\varepsilon_0 L / \ln(4h/d)$, where ε_0 is the dielectric constant, $\varepsilon = 2.45$ is the average of the dielectric constants of vacuum and SiO_2, h is the dielectric thickness, L is the length of the tube, and d is the CNT diameter. Spectrum of noise from a CNT FET at a bias voltage shown on linear-linear scale (main panel) and log-log scale (inset) is shown in Fig. 7. The value of the Hooge parameter $\alpha(T)$ can then be determined from the slope of the $\langle 1/A \rangle$ versus V_g plot (Fig. 8), which is equal to $C_g / e\alpha(T)$. Note that extraction of $\alpha(T)$ is insensitive to changes in carrier number caused by, e.g., changes in the threshold voltage with temperature. Authors discussed the peak in $D(E)$ at $E \sim 0.4$ eV and argue that this feature, i.e., the broad peak that ranges from -0.2 to 0.6 eV, is responsible for the majority of the room temperature noise. The low-energy behavior of $D(E) \sim 1/E$ corresponds to an approximately temperature-independent Hooge parameter. Thus, the rise of the Hooge parameter by a factor of ~20 from low temperature to room temperature is due entirely to the broad peak in $D(E)$ around 0.4 eV. The characteristic energy scale allows us to rule out some possibilities for the source of the noise. The energy scale is comparable to the band gap (~0.5 and ~0.37 eV for devices 1 and 2, respectively) and, therefore, one can rule out electronic excitations (e.g., defect ionization, etc.) within the CNT itself as the major noise source; such mechanisms should have characteristic energies less than or equal to half the band gap. Temperature dependence of the Hooge parameter and distribution of activation energies of the fluctuators $D(E)$ was presented in Fig.9.

A RTS appears at a smaller absolute gate bias for a larger absolute drain-source bias in a CNT transistor [36]. Its mechanism is attributed to a defect located in the drain side of the Schottky barrier CNT transistor with Ti/Au as contact material. It is note that room temperature RTS is presented for both metallic and s-CNT. In [36] a correlated RTS is observed from the

interaction of two individual defects in a CNT. It is shown that the amplitude fluctuation of one defect significantly depends on the state of the other defect. Moreover, statistics of the correlated switching is shown to deviate from the ideal Poisson process. Physics of this RTS correlation is attributed to the fact that the two defects are located closer than the sum of their Fermi-Thomas screening lengths. The switching of resistance between two discrete values, known as RTN, was observed in individual carbon SWNT [74]. The RTN has been studied as a function of bias-voltage and gate-voltage as well as temperature. By analyzing the features of the RTN, authors identify three different types of RTN existing in the SWNT related systems. While the RTN can be generated by the various charge traps in the vicinity of the SWNTs, the RTN for metallic SWNTs is mainly due to reversible defect motions between two metastable states, activated by inelastic scattering with electrons [74].

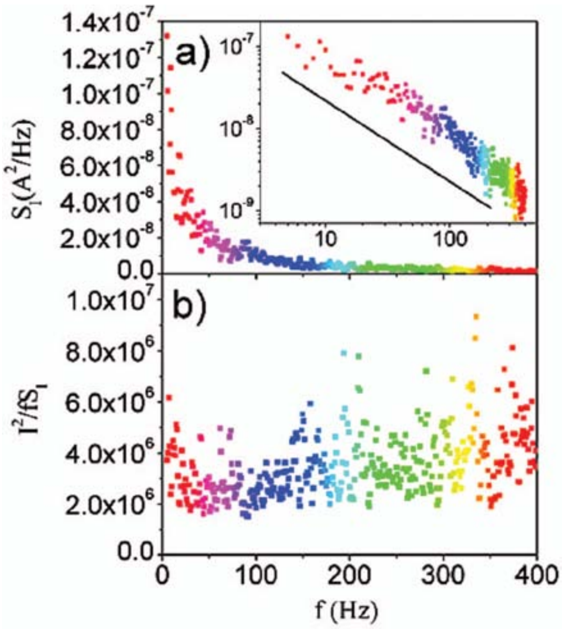

Fig. 7. (a) Spectrum of 1/*f*-noise from a CNT FET at a bias voltage of 100 mV with each frequency point color coded a gate voltage of −8V, and a temperature of 150 K, shown on linear-linear scale (main panel) and log-log scale (inset). The color coding is consistent from Fig. 7 to Fig. 8 and allows the display of the frequency information in the next figure. The solid line in the inset indicates a slope of −1. (b) Presentation of the data to show the value of $1/A = I^2/fS_I$ at each frequency [73].

Due to the geometrical complexity of NT networks in the channel area and the large number of tube–tube/tube–metal junctions, the 1/f-dependence of the noise shows a similar level to that of a single SWNT transistor. Detailed analysis is performed with the parameters of number of mobile carriers and mobility in the different environment. This shows that the change in the number of mobile carriers resulting in the mobility change due to adsorption and desorption of gas molecules (mostly oxygen molecules) to the tube surface is a key factor in the 1/f-noise level for CNT network transistors [75].

In [49] reported on the 1/f-noise in various ballistic CNT devices. By contacting semiconducting tubes with different metal electrodes it is shown that a small A/R value by itself is no indication of a suitable metal/tube combination for logic applications. Here discussed how current in a NT transistor is determined by the injection of carriers at the electrode/NT interface, while at the same time excess noise is related to the number of carriers inside the NT channel. It is demonstrate a substantial reduction in noise amplitude for a tube transistor with multiple CNTs in parallel.

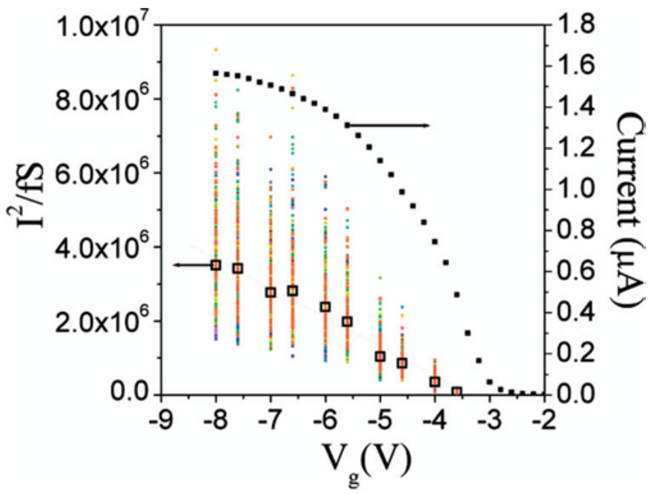

Fig. 8. Reciprocal of the noise pre-factor $1/A = I^2/fS_I$ (colored squares) and current (filled squares) versus gate voltage for device 1 at 150 K. Current data are taken with source-drain voltage of 100 mV. The $1/A$ data are color coded to indicate frequency as in Fig. 7. The open squares indicate the mean values of $\langle 1/A \rangle$ at each gate voltage, and the dotted line is a linear fit to these points. The standard deviation of the mean for these points is smaller than the size of the boxes used to indicate the mean value. Note that larger $1/A$ values correspond to less noise [73].

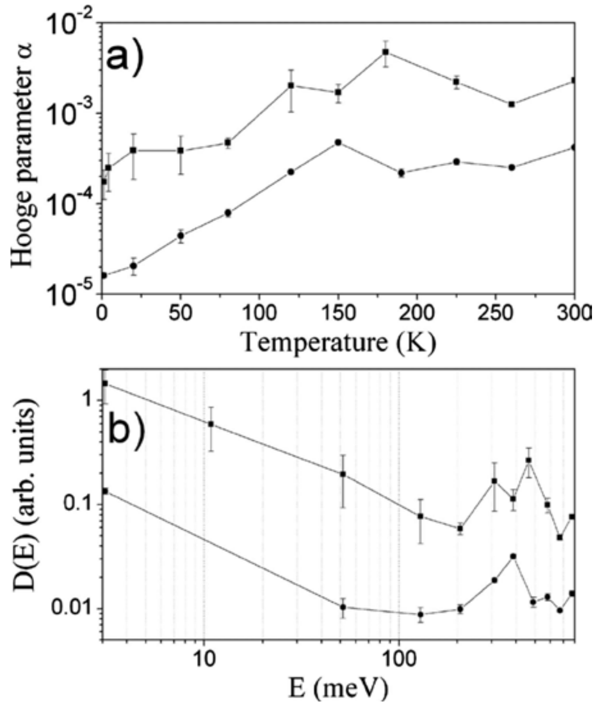

Fig. 9. (a) Temperature dependence of the Hooge parameter $\alpha(T)$ for both CNT devices. The data points are calculated using the slope from $\langle 1/A \rangle$ vs. V_g, as shown in Fig.8. The significant upward trend between 1.2 K and about 150 K is seen in both samples. (b) Distribution of activation energies of the fluctuators $D(E)$ responsible for 1/f-noise, calculated as described in the text. Filled squares and circles correspond to device 1 and device 2, respectively, in both (a) and (b) [73].

Using a semi-classical approach, it has been shown by R. Landauer that the conductance in a low-dimensional system with ballistic transport could be expressed as [76]

$$G = \left(2e^2/h\right)MP\,, \tag{22}$$

where P is the average probability of an electron being transmitted along the conductor. M (= 2 for SWNT) is the number of electronic sub-bands which participate to the conduction [77]. In ballistic transport ($P = 1$), the intrinsic resistance of the conductor is zero but interactions between electrons or electron-phonon coupling can affect the intrinsic resistance of the tube. Nevertheless, the conductance has a finite value given by $4e^2/h$, involving an intrinsic contact resistance of 6.5 $\mathrm{k\Omega}$ [76,78]. This value has been almost reached in metallic NTs samples with low contact resistances and in s-NTs with the use of a gate bias [79,80].

Low-frequency noise measurements on individual SWCNT transistors exhibiting ambipolar characteristics have been carried out [111]. With a polymer electrolyte as gate medium, low-frequency noise can be monitored in both p- and n-channel operation of the same nanotube under the same chemical environment. 1/f-noise in the p-channel of polymer electrolyte gated nanotube transistor is similar to that of back gate operation. Most devices exhibit significantly larger noise amplitude in the n-channel operation that has a distinct dependence on the threshold voltage. A nonuniform energy distribution of carrier trapping/scattering sites is considered to explain these observations [111].

3. Si, GaAs and other materials based NTs and NWs

Silicon NWs are among the most promising one-dimensional nanomaterials for future nanoelectronic devices [17,81]. Both p- and n-doping of Si NWs can be achieved controllably, and Si NWs are compatible with existing high volume Si manufacturing processes [82]. For future applications, the control of key FET parameters such as p- or n-type, threshold voltage, on/off ratio, and channel mobility is crucial. Most Si NW FETs utilize metals as source and drain and operate in accumulation mode; a gate bias is required to generate majority carriers. It is well accepted that the characteristics of the latter are controlled by Schottky barriers between metal and conducting channels [29,83]. In [81] reported the results of systematic annealing to control the properties of metal source and drain contacts to Si NW, and process optimization to achieve high performance ambipolar Si NW FETs.

The schematic diagram depicting the sample preparation method of amine-functionalized Si-NW suspensions and the large-scale assembly method of Si NW-based integrated devices is presented in Fig.10.

The electric-field-induced optical spectral changes of SWNT films using a TFT configuration was reported in [85]. Under the gate electric field, the spectra of the SWNTs displayed continuous intensity modulation. These results provided evidence of carrier accumulation in SWNT-TFTs. The amount of accumulated carriers was quantitatively consistent with the carrier density in the nanoscale wire-form FET model. The device was fabricated on the base of heavily doped n-Si wafer, with a 400 nm thick insulating SiO_2 layer, was used for the bottom electrode. Comb-shaped drain and source electrodes of 10/100 nm thick Cr/Au, respectively, were fabricated on the surface of the SiO_2 layer. Finally, SWNTs were suspended in N, N-dimethylformamide and deposited. thickness of the TFT was 25 nm.

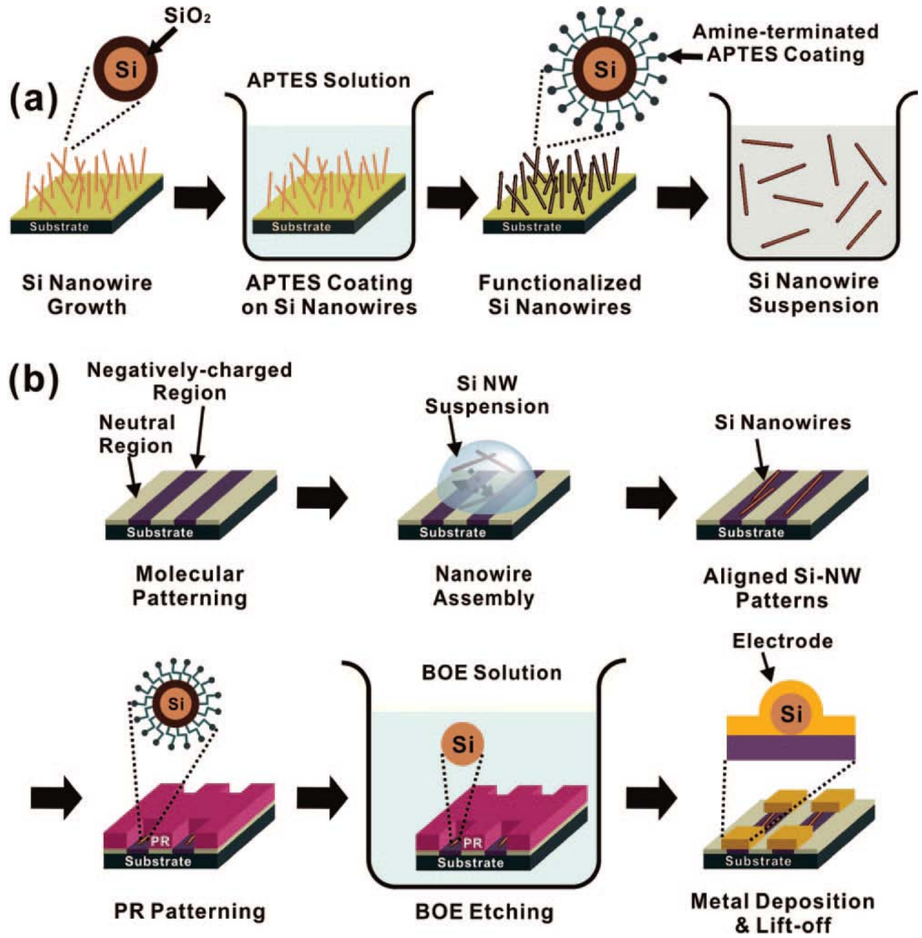

Fig. 10. (a) Schematic diagram depicting the sample preparation method of amine-functionalized Si-NW suspensions. (b) Schematic diagram depicting the large-scale assembly method of Si-NW-based integrated devices [84].

LF noise measurement was carried out to study the current fluctuations in Si NW-based devices [84]. The device exhibited a $S_I \sim 1/f^{\gamma}$ noise spectrum with γ values in the range of 0.85–1.3, indicating a typical 1/f-behavior [2,86]. The noise behavior was characterized using empirical Hooge's relationship (2). The Hooge's parameter for typical bulk materials and NTs is of the order of 10^{-3}. On the other hand, low-noise Si devices and best condition Si NWs have the Hooge's parameter in the range of 10^{-3}-10^{-6} [87-89]. The calculated Hooge's parameter of Si NW FETs is 5.34×10^{-3}, indicating noise level similar to typical NT-based devices though it was worse than low-noise Si-based devices. In [88] the I-V and noise characteristics of bridging Si wires have been measured at 300K. From the linear I-V characteristics the bulk and contact resistance contributions are extracted and modeled. The excess noise observed at LF is interpreted in terms of bulk and contact noise contributions, with the former comparable, in terms of Hooge parameter values, to the low noise levels observed in high-quality Si devices. The contact noise is significant in some devices and is attributed to the impinging end of the bridging NWs.

Some of the inherent challenges and limitations of exploiting nanomaterial resistive sensors for gas detection due to noise and process variation are described in [90]. In the context of energy-harvesting wireless sensor networks, the opportunities and limits of circuit techniques to compensate for some sensor non-idealities are discussed. Si NW FET conductance signals recorded from cardiomyocytes exhibited excellent SNR with values routinely >5 and signal amplitudes that were tuned by varying device sensitivity through changes in the gate-voltage potential [91].

GaN is a very attractive semiconductor. It has allowed a revolution in the field of blue and white LEDs as well as for microwave power applications. This is mainly due to its large band gap that is more than tripled as compared to silicon and more than doubled as compared to GaAs. GaN allows the realization of AlGaN/GaN heterostructures. This heterojunctions contains an internal polarization field that induces the presence of a 2D electron gas without intentional doping. High breakdown voltages, electron mobilities, and carrier densities can be achieved, which have allowed the realization of microwave amplifiers with record power [92]. GaN NWs are therefore of strong interest. A significant volume of work on the FET behavior of GaN NWs has been carried out in the past years [93-100]. GaN NWs in particular have shown potential for a wide range of optical and electronic applications. Room-temperature UV lasing has been reported for GaN NW systems [101]. GaN NW FETs [102] and logic devices [28] have shown desirable characteristics such as high transconductance and good switching.

A comparative study is presented of LF noise in GaN-based MOS heterostructure FETs (MOS-HFETs) and HFETs [21]. The Hooge parameter at zero gate bias was of the order of 10^{-3} for both types of device. AlGaN/GaN MOS-HFETs exhibited extremely low gate leakage current and much lower noise at both positive and negative gate biases. It is shown that the level of 1/f- and g-r noise in GaN NW FETs can be suppressed by UV radiation by up to an order of magnitude [22]. This strong suppression of the noise is explained by the illumination changing the occupancy of traps responsible for noise. Investigations of the noise properties of GaN NWs in [19,20,103] show that the 1/f-noise arises due to the relaxation of the defects or the dynamics of groups of defects in a finite relaxation time. It is indicated that the 1/f-noise is the noise which is relative to the frequency

$$S_V = \alpha \frac{V^{2+\delta}}{N f^{\gamma}} \tag{43}$$

only when $\gamma = 1$ and $\delta = 0$, $\alpha = 2\times10^{-3}$ in metal and semiconductor [1-3,65].

In [19,20,103] measured the 1/f-noise for the frequency below 50Hz. Results show that the GaN NWs also exhibit the 1/f-like excess noise. Authors note that the 1/f-noise of the NWs exists in a LF range than that of the CNTs**.**

The Hooge parameter is obtained from the data between 0.5 Hz and 8 Hz. For $R = 34.205$ kΩ the average Hooge parameter is 1.007± 0.045 in $I > 30$ nA. For $R = 872.866$ kΩ the average Hooge parameter of the samples is 1.097± 0.084 in $I > 0.835$ nA. Comparing the noise of the metal film resistor with the noise of the GaN NWs, the GaN NWs clearly exhibit the excess 1/f-noise. The smaller resistant of the GaN NW is the lower frequency of the 1/f-noise is exhibited in. 1/f-noise of the GaN nanowire in the current range 0.1nA – 100nA was measure. In the bandwidth from 0.5Hz to 8Hz at the room temperature, the Hooge parameter is very close to one. In [104] reported on the fabrication and characterization of high electron mobility transistor structures based on epitaxially grown AlGaN/GaN layers. The LF noise spectra were measured at different temperatures in the range from 70 to 290 K. UV excitation was used to restore trap states after treatment of the structures at a high applied voltage. The noise spectra follow $1/f^{\gamma}$ dependence with $\gamma \sim 1$ for structures with wide and nanoscale widths. The LF noise temperature behavior in [160] explained using a charge fluctuation model. Noise behavior explained by taking into account a decrease in the internal dimension of the wires which strengthening by surface depletion resulting in a quantization of the electron energy and a transformation of the 2D confinement to a 1D confined system. In this case exchange between the conducting channel and the defects in the depletion layers in noise level and an increase in channel effective conductivity.

An alternative to the oxide-based FET approach is the MESFET, which uses a Schottky barrier in place of the insulating oxide. Effective Schottky gating has previously been demonstrated in MESFETs made from single CdS nanobelts and ZnO nanorods [105,106]. A heterojunction of n-type ZnO NWs and p-Si has been successfully constructed to demonstrate UV photodiodes [107]. The I-V characteristics show the typical rectifying behavior of heterojunctions, and the photodiode exhibits response of ~0.07 A/W for UV light (365 nm) under a 20 V reverse bias.

A heterojunction of n-ZnO NWs and p-Si has been successfully constructed to demonstrate UV photodiodes [107]. The prototype device consists of naturally doped n-ZnO NWs grown on top of a (100) p-Si substrate by the bottom-up growth process. The diameter of the NWs is in the range of 70–120 nm, and the length is controlled by the growth time. The isolation is achieved by using spin-on glass that also works as the foundation of the top electrode. In [23] was investigated bending-induced enhancement in the conductance of individual ZnO NWs or CdS nanobelts. I-V characteristics of ZnO NWs are symmetrical and linear.

The characteristics of LF noise in the drain current of n-type ZnO FETs have been investigated through RTSs at 4.2 K [24]. At room temperature, the noise power spectra have classic 1/f-dependence with a Hooge parameter that is ~5×10^{-3}. At 4.2 K, the device's noise spectra change from 1/f to Lorentzian type, and the current traces as a function of time show RTSs. The channel current RTSs are attributed to correlated carrier number and mobility fluctuation due to the trapping and emission of carriers by discrete border traps.

The excess noise in single crystal systems can be due to the defect diffusion along the dislocations, movement of dislocations, etc., which are highly crystal structure dependent. To study the effect of defect dynamics on electrical noise in single-crystalline NWs, in [108] have used silver NWs realized in both hcp and fcc crystal structures. In [108] employed a modified electrodeposition technique in which an inter-electrode potential, much smaller than the Nernst potential, was applied across a highly concentrated electrolyte and the resulting NWs acquired hcp structure. Electrical noise was measured with ac multiprobe technique in an electromagnetically shielded set-up that is sensitive to voltage fluctuations with power spectral densities as low as 10^{-20} V^2/Hz. It is found that the noise magnitude at room temperature in fcc NWs is three orders of magnitude higher than that of hcp NWs. The observed temperature-independent behavior of noise in hcp silver NWs can be explained in terms of locking of dislocation motion [108].

4. Conclusion

Thus, on the base of the investigations of electrical, physical, chemical and other characteristics of NTs and NWs we can have some conclusions:

a. NTs and NWs are promising candidates for advanced nanoelectronic devices, and they have great potential in a wide range of applications, such as FETs, elementary logic circuits, bio- and chemical sensors, nanotechnology, biotechnology, electronics, memory devices, optics and other fields of materials science, as well as potential uses in architectural fields.

b. LF noise spectral density is expressed as

$$S_V = A\frac{V^{2+\beta}}{f^{\gamma}}.$$

c. Parameter A generally reflects the sample quality and increases with decreasing device size and depends on many parameters of material, its structure, sizes, NTs bulk and surface physical and chemical conditions, from its fabrication method. The noise amplitude

$$A \propto R,\ A \propto \frac{1}{N},\ A = \frac{\alpha_H}{N},\ A \propto \frac{1}{L},$$

R is the device resistance, N is the number of atoms or carriers in the system, L is the sample length ($N \propto L$). $A = 1.0\times10^{-11} R$. Parameter A vary within 10^{-13} up to 4×10^{-4}.

d. Parameter $\beta = 0$ is expected for pure resistance fluctuation in ohmic conductors. The $\gamma \neq 1$ behavior is associated with nonlinear characteristics. Usually $|\beta| << 1$, $|\Delta\gamma| << 1$ are material-dependent numbers ($\gamma = 1 + \Delta\gamma$).

e. Excess noise with a slope different from unity ($\gamma \neq 1$) can be explained by a superposition of a few Lorentzians and of the 1/f-noise. The change in slope with respect to temperature is thus explained by the variation of trap activities.

f. Investigation of noise sources and its behavior will be powerful source for determination and explanation of physical processes in NTs and NWs and will help us to suggest noise reduction method for NT based devices.

REFERENCES

1. **F.N.Hooge,** Phys. Lett. A, **29**, 139 (1969).
2. **F.N.Hooge, T.G.M. Kleinpenning, L.K.J. Vandamme,** Rep. Prog. Phys., **44**, 479 (1981).
3. **F.N.Hooge,** IEEE Trans. Electron Devices, **41**, 1926 (1994).
4. **K.Hung, P.Ko, C.Hu, Y.Cheng,** IEEE Trans. Electron Devices, **37**, 654 (1990).
5. **J.Mannik, I.Heller, A.M.Janssens, S.G.Lemay, C.Dekker,** Nano Lett., **8(2)**, 685 (2008).
6. **M.N.Mihaila,** Fluctuation Noise Lett., **4**, L329 (2004).
7. **F.V.Gasparyan, H.V.Asriyan, S.V.Melkonyan C.E. Corman,** U.S. Patent Application for Letters Patent of the United States No. 61/332,408.
8. **G.Ghibaudo, T.Boutchacha,** Microelectron. Reliab., **42**, 573 (2002).
9. **P.G.Collins, M.S.Fuhrer, A.Zettl,** Appl. Phys. Lett., **76(7)**, 894 (2000).
10. **M.F.G.Hedouin, P.J.Rous,** Phys. Rev. B, **62**, 8473 (2000).
11. **A.Bid, A.Bora, A.K.Raychaudhuri,** Phys. Rev. B, **72**, 113415 (2005).
12. **H.W.Ch.Postma, T.F.Teepen, Z.Yao, C.Dekker,** Proc. XXXVI-th Rencontres de Moriond, EDP Sciences, France, 2001.
13. **P.-E.Roche, M.Kociak, S.Gueron, A.Kasumov, B.Reulet, H.Bouchiat,** Eur. Phys. J. B, **28**, 217 (2002).
14. **E.S.Snow, J.P.Novak, M.D.Lay, F.K.Perkins,** Appl. Phys. Lett., **85(18)**, 4172 (2004).
15. **Y.-M.Lin, J.Appenzeller, J.Knoch, Z.Chen, P.Avouris,** Nano Lett., **6(5)**, 930 (2006).
16. **M.Ishigami, J.H.Chen, E.D.Williams,** Appl. Phys. Lett., **88**, 203116(1-3) (2006).
17. **Y.Cui, C.M.Lieber,** Science, **291**, 851 (2001).
18. **F.V.Gasparyan, A.Poghossian, S.A.Vitusevich, M.V.Petrychuk, V.A.Sydoruk, A.V.Surmalyan, J.R.Siqueira Jr., O.N.Oliveira Jr., A.Offenhäusser, M.J.Schöning,** Proc. 20th Int. Conf. Fluctuation and Noise, 14-19 June, Pisa, Italy. 2009, pp.133-136.
19. **P.Dutta, P.M.Horn,** Rev. Mod. Phys., **53**, 497 (1981).
20. **H.Ouacha, M.Willander, H.Y.Yu, Y.W.Park, M.S.Kabir, S.H.Magnus Persson, L.B.Kish, A.Ouacha,** Appl. Phys. Lett., **80**, 1055 (2002).

21. **P.N.Rumyantsev, M.S.Shur, M.A.Khan, et al.,** Electronics Letters, **36(3)**, 268 (2000).
22. **S.L.Rumyantsev, M.S.Shur, et al.,** J. Appl. Phys., **103**, 064501 (2008).
23. **F.Pascal, S.Jarrix, C.Delseny, G.Lecoy, T.Kleinpennng,** J. Appl. Phys., **79(6)**, 3046 (1996).
24. **H.D.Xiong, W.Wang, Q.Li, et al.,** D.M.Fleetwood, Appl. Phys. Lett., **91**, 053107 (2007).
25. **S.J.Tans, A.R.M.Verschueren, C.Dekker,** Nature, **393**, 49 (1998).
26. **R.Martel, T.Schmidt, H.R.Shea, T.Hertel, Ph.Avouris,** Appl. Phys. Lett., **73**, 2447 (1998).
27. **Y.Cui, Z.Zhong, D.Wang, W.U.Wang, C.M.Lieber,** Nano Lett., **3**, 149 (2003).
28. **Y.Huang, X.Duan, Y.Cui, L.J.Lauhon, K.H.Kim, C.M.Lieber,** Science, **294**, 1313 (2001).
29. **V.Derycke, R.Martel, J.Appenzeller, Ph.Avouris,** Appl. Phys. Lett., **80(15)**, 2773 (2002).
30. **A.Bachtold, P.Hadley, T.Nakanishi, C.Dekker,** Science, **294**, 1317 (2001).
31. **X.Liu, C.Lee, C.Zhou, J.Han,** Appl. Phys. Lett., 79, 3329 (2001).
32. **J.Kong, N.R.Franklin, C.Zhou, M.G.Chapline, S.Peng, K.Cho, H.Dai,** Science, **387**, 622 (2000).
33. **Y.Cui, Q.Wei, H.Park, C.M.Lieber,** Science, **293**, 1289 (2001).
34. **E.S.Snow, F.K.Perkins, E.J.Houser, S.C.Badescu, T.L.Reinacke,** Science, **307**, 1942 (2005).
35. **L.Roschier, R.Tarkiainen, et al.,** Appl. Phys. Lett**., 78,** 3295 (2001).
36. **F.Liu, K.L.Wang, D.Zhang C.Zhou,** Appl. Phys. Lett., **89**, 243101 (2006).
37. **M.S.Fuhrer, B.M.Kim, T.Durkop, T.Brintlinger,** Nano Lett., **2**, 755 (2002).
38. **M.Radosalvljevic, M.Freitag, K.V.Thadani, A.T.Johnson,** Nano Lett., **2**, 761 (2002).
39. **T.Durkop,** Ph.D. thesis, University of Maryland at College Park, 2004.
40. **P.G.Collins, K.Bradley, M.Ishigami, A.Zettl,** Science, **287**, 1801 (2000).
41. **R.Vajtai, B.Q.Wei, Z.J.Zhang, Y.Jung, et al.,** Smart Mater. Struct., **11**, 691 (2002).
42. **I.Heller, J.Mannik, S.G.Lemay, C.Dekker,** Nano Lett., **9(1)**, 377 (2009).
43. **R.Tarkiainen, L.Roschier, M.Ahlskog, M.Paalanen, P.Hakonen.** Physica E, **28**, 57 (2005).
44. **P.Dutta, P.M.Horn,** Rev. Mod. Phys., **53**, 497 (1981).
45. **M.Briman, K.Bradley, G.Gruner,** J. Appl. Phys., **100**, 013505(1-5) (2006).
46. **Y.-M.Lin, J.Appenzeller, Z.Chen, P.Avouris,** Physica E, **37**, 72 (2007).
47. **Y.-M.Lin, J.C.Tsang, M.Freitag, P.Avouris,** Nanotechnology, **18**, 295202(1-6) (2007).
48. **B.W.Jacobs, V.M.Ayres, M.A.Tupta, et al.,** Electronic Transport Characteristics of Gallium Nitride Nanowire-based Nanocircuits, 2006 6th IEEE Conference on Nanotechnology Proceedings, ISBN 1-4244-0078-3
49. **J.Appenzeller, Y.M.Lin, J.Knoch, et al.,** IEEE Trans. On Nanotechnology, **6(3)**, 368 (2007).
50. **J.Tersoff,** Nano Lett., **7(1)**, 194 (2007).
51. **S.Rossenblatt, Y.Yaish, J.Park, J.Gore, V.Sazonova, P.L.McEuen,** Nano Lett., **2(8)**, 869 (2002).
52. **S.Soliveres, A.Hoffmamm, F.Pascal, et al.,** Fluctuation and Noise Letters, **6(1)**, L45 (2006).
53. **H.V.Asriyan, F.V.Gasparyan, V.M.Aroutiounian,** Proc. SPIE's 1st Int. Symp. on Fluctuation and Noise. 1-4 June 2003, Santa Fe, New Mexico USA, **vol. 5115**, pp. 401-411.
54. **S.V.Melkonyan, F.V.Gasparyan, V.M.Aroutiounian, C.E.Korman,** Proc. SPIE's 1st Int. Symp on Fluctuation and Noise. 1-4 June 2003, Santa Fe, New Mexico USA, V.5115, pp. 412-420.

55. **H.V.Asriyan, F.V.Gasparyan, V.M.Aroutiounian, S.V.Melkonyan, P.Soukiassian,** Sensors and Actuators A, **113**, 338 (2004).
56. **H.V.Asriyan, F.V.Gasparyan,** Modern Physics Letters B, 18(10), 427 (2004).
57. **S.V.Melkonyan, V.M.Aroutiounian, F.V.Gasparyan, C.E.Korman,** Physica B: Physics of Condensed Matter, **357(3-4)**, 398 (2005).
58. **H.V.Asriyan, A.A.Shatveryan, V.M.Aroutiounian, F.V.Gasparyan, S.V.Melkonyan, Z.H.Mkhitharian, G.Ayvazyan,** Noise and Information in Nanoelectronics, Sensors, and Standards part of SPIE's 3rd Int. Symp. on Fluctuations and Noise, 24-26 May 2005, Austin, Texas USA, v.5846-25, 2005, pp.192-199.
59. **S.V.Melkonyan, V.M.Aroutiounian, F.V.Gasparyan, H.V.Asriyan,** Physica, B: Physics of Condensed Matter, **382(1-2)**, 65 (2006).
60. **F.V.Gasparyan, S.V.Melkonyan, H.V.Asriyan,** BPU-6 Conference Istanbul, Turkey, 22–26 August, 2006, p.601.
61. **S.V.Melkonyan, F.V.Gasparyan, H.V.Asriyan,** SPIE 4th Int. Symp. Fluctuation and Noise, ay 2007, Florence, Italy, Proceedings of SPIE, **6600**, 2007, pp.66001K-1–66001K-8.
62. **S.V.Melkonyan, F.V.Gasparyan, V.M.Aroutiounian, H.V.Asriyan,** 18th Int. Conf. on Noise and Fluctuations (ICNF 2005) September 19-23, 2005, Salamanca, Spain, 780, pp.87-91.
63. **M.N.Mihaila,** in Noise and Fluctuations Control in Electronic Devices; Balandin,A., ed.; American Science Publishers: Stevenson Ranch, CA, 2002, Chapter 18, pp.366-385.
64. **A.Behnam, A.Ural, G.Bosman,** Proc. 20th Int. Conf. on Noise and Fluctuations, Pisa, Italy, 14-19 June, 2009. NY 2009, pp.79-84.
65. **A.Behnam, A.Ural,** Phys. Rev. B, **75**, 125432(1-8) (2007).
66. **S.Soliveres, F.Martinez, A.Hoffmann,** F.Pascal, Proc. 20th Int. Conf. on Noise and Fluctuations, Pisa, Italy, 14-19 June, 2009 NY 2009, pp. 85-88.
67. **H.Akabane, N.Miwa,** Proc. 20th Int. Conf. on Noise and Fluctuations, Pisa, Italy, 14-19 June, 2009, NY 2009, pp. 483-486.
68. **F.Liu, M.Bao, H.Kim, K.L.Wang, C.Li, X.Liu, C.Zhou,** Appl. Phys. Lett., **86**, 163102(1-3) (2005).
69. **Z.Yao, C.Dekker, P.Avouris,** Carbon Nanotubes: Synthesis, Structure, Properties and Application. New York, Springer, 2002, p.147.
70. **L.K.J.Vandamme, X.Li, D.Rigaud,** IEEE Trans. Electron Devices, **41**, 1936 (1994).
71. **M.S.Gudiksen, L.J.Lauhon, J.Wang, D.C.Smith, C.M.Lieber,** Nature, **415**, 617 (2002).
72. **Y-M.Lin, J.Appenzeller,** Ph.Avouris, Nano Lett., **4**, 947 (2004).
73. **D.Tobias, M.Ishigami, A.Tselev, et al.,** Phys. Rev. B, **77**, 033407(1-4) (2008).
74. **S.H.Jhang, S.W.Lee, D.S.Lee, E.B.Campbell, S.Roth, Y.W.Park,** MRS, **7(15)** (2009).
75. **U.J.Kim, K.H.Kim, K.T.Kim, Y.-S.Min, W.Park,** Nanotechnology, **19**, 285705(1-4) (2008).
76. **S.Datta,** Electronic Transport in Mesoscopic Systems, Cambridge University Press, Cambridge, 1995.
77. **M.Anantram, L.Delzeit, A.Cassell, J.Han, M.Meyyappan,** Physica E, **11**, 118 (2001).
78. **A.Svizenko, M.P.Anantram, T.R.Govindan,** IEEE Trans. Nanotechnol., **4**, 557 (2005).

79. **A.Javey, J.Guo, D.B.Farmer, et al.,** Nano Letters, **4(7)**, 1319 (2004).
80. **A.Javey, J.Guo, Q.Wang, M.Lundstrom, H.Dai,** Nature, **424**, 654 (2003).
81. **K.Byon, D.Tham, J.E.Fischer, A.T.Johnson,** Appl. Phys. Lett., **90(5)**, 143513(1-3) (2007).
82. **G.Zheng, W.Lu, S.Jin, C.M.Lieber,** Adv. Mater. (Weinheim, Ger.), **16**, 1890 (2004).
83. **F.Leonard, J.Tersoff,** Phys. Rev. Lett., **84**, 4693 (2000).
84. **K.Heo, E.Cho, J.-E.Yang, M.-H.Kim, et al.,** Nano Lett., **8(12)**, 4523 (2008).
85. **T.Takenobu, Y.Murayama, M.Shiraishi, Y.Twasa,** Japanese J. of Appl. Phys., **45(45)**, L1190 (2006).
86. **W.Y.Wang, H.D.Xiong, M.D.Edelstein, et al.,** J. Appl. Phys., **101**, 044313 (2007).
87. **H.Mikoshiba,** IEEE Trans. Electron Devices, **29**, 965 (1982).
88. **S.Reza, G.Bosman, A.S.Islam, T.I.Kamins, et al.,** IEEE Trans. Nanotechnol., **5**, 523 (2006).
89. **J.Lee, B.Y.Yu, I.Han, K.J.Choi, G.Ghibaudo,** J. Nanoscience and Nanotechnology, **8(10)**, 5257 (2008).
90. **R.Amirtharajah, A.Chen, J.Loo, N.J.Guilar,** Int. J. of Nanotechnology, **5(4-5)**, 497 (2008).
91. **T.Cohen-Karni, B.P.Timko, L.E.Weiss, C.M.Lieber,** Appl. Biological, **106(18)**, 7309 (2009).
92. **U.K.Mishra, L.Shen, T.E.Kazior, Y.-F.Wu,** Proc. IEEE, **96(2)**, 287 (2008).
93. **H.Y.Cha, H.Q.Wu, S.Chae, M.G.Spencer,** J. Appl. Phys., **100(2)**, 024307(1-4) (2006).
94. **H.Y.Cha, H.Q.Wu, M.Chandrashekhar, et al.,** Nanotechnology, **17(5)**, 1264 (2006).
95. **W.Huaqiang, C.Ho-Young, M.Chandrashekhar, et al.,** J. Electron. Mater., **35(4)**, 670 (2006).
96. **S.Y.Lee, T.H.Kim, D.I.Suh, N.K.Cho, et al.,** Chem. Phys. Lett., **427(1-3)**, 107 (2006).
97. **A.Motayed, M.Vaudin, A.V.Davydov, et al.,** Appl. Phys. Lett., **90(4)**, 043104(1-3) (2007).
98. **L.Sang-Kwon, S.Han-Kyu, C.Ki-Chul, et al.,** Mater. Sci. Forum, **527–529**, 1549 (2006).
99. **E.Stern, G.Cheng, E.Cimpoiasu, R.Klie, S.Guthrie, et al.,** Nanotechnology, **16(12)**, 2941 (2005).
100. **H.Yu, D.Xiangfeng, C.Yi, C.M.Lieber,** Nano Lett., **2(2)**, 101 (2002).
101. **J.Johnson, H.J.Choi, K.P.Knutsen, R.D.Schaller, P.Yang, R.J.Saykally,** Nat. Mater., **1**, 101 (2002).
102. **Y.Huang, X.Duan, Y.Cui, C.M.Lieber,** Nano Lett., **2**, 101 (2002).
103. **A.K.Raychaudhuri,** Curr. Opin. Solid State Mater. Sci., **6**, 67 (2002).
104. **S.A.Vitusevich, M.V,Petrichuk, V.A.Sydoruk,** Proc. 20th Int. Conf. on Noise and Fluctuations, Pisa, Italy, 14-19 June, 2009, NY 2009, pp. 487-490.
105. **R.M.Ma, L.Dai, G.G.Qin,** Nano Lett., **7(4)**, 868 (2007).
106. **W.I.Park, J.S.Kim, G.C.Yi, H.J.Lee,** Adv. Mater., **17(11)**, 1393 (2005).
107. **L.Luo, Y.Zhang, S.S.Mao, L.Lin.** Sensors and Actuators A, **127**, 201 (2006).
108. **A.Singh, A.Ghosh,** MRS Symposium JJ: Proc., vol. 1142. Nanotubes, Nanowires, Nanobelts, and Nanocoils. Boston, December 1–4, 2008. Paper JJ15.11.
109. **F.V.Gasparyan, A.Poghossian, S.A.Vitusevich, M.V.Petrychuk, V.A.Sydoruk, J.R.Siqueira Jr., O.N.Oliveira Jr., A.Offenhäusser, M.J.Schöning,** IEEE Sensors Journal, 2010 (in press).
110. **F.V.Gasparyan, Z.H.Mkhitaryan, A.V.Surmalyan,** Proc. 7th Int. Conf. Semicond. Micro. & Nanoelectronics, Tsakhcadzor, Armenia, July 3–5, 2009, pp.101-104.
111. **J.H.Back, K.Sunkook, M.Saeed, S.Moonsub,** Nano letters, **8(4)**, 1090 (2008).